JOURNAL OF APPLIED POLYMER SCIENCE VOL. 21, 141–148 (1977)

Filler Structure and Tensile Properties of Starch Xanthide-Reinforced Vulcanizates

R. J. DENNENBERG, R. A. BUCHANAN, and E. B. BAGLEY, *Northern Regional Research Laboratory, Agricultural Research Service, U.S. Department of Agriculture, Peoria, Illinois 61604*

Synopsis

Stress–strain behavior of some starch xanthide- and carbon black-reinforced styrene–butadiene elastomers was investigated as a function of filler particle size and structure. In starch xanthide systems, low strain behavior is sensitive to particle structure; high strain behavior, to particle size. Electron photomicrographs of the several starch xanthide-reinforced vulcanizates were analyzed with reference to filler particle size and structure. These parameters were then correlated with Mooney plots of [load/$\lambda - \lambda^{-2}$] versus λ^{-1}, where λ is the strain ratio. Plots of samples containing highly structured filler particles were highly nonlinear, rising steeply as λ^{-1} approached unity. Samples containing nonstructured filler particles were also highly nonlinear, rising steeply as λ^{-1} decreased to approximately 0.4. A preliminary study of the dynamic properties of these samples, as determined in an eccentric rotating-disk rheometer, provided little additional information.

INTRODUCTION

Coprecipitation of starch xanthide with a variety of elastomers (e.g., nitrile, styrene–butadiene (SBR), and natural rubber) was first reported by Buchanan et al.[1,2] and by Stephens et al.[3] Initially, elastomer latex is dispersed in a starch xanthate solution at pH 11 or above. Acidification under oxidizing conditions brings about the simultaneous precipitation of elastomer and starch xanthide, the product being in the form of elastomer encased in swollen crosslinked starch xanthide. Subsequent drying and high shear mastication of the coprecipitate reverse the phases to give starch xanthide dispersed in elastomer.[4]

The starch xanthide can be in the form of rigid particles,[4] or it can be distributed throughout the rubber as a structured network.[5] In either event, the rigid starch xanthide acts as an effective reinforcing agent so that, for example, an SBR vulcanizate reinforced with 43 parts per hundred rubber by weight (phr) starch xanthide will exhibit ultimate tensile strengths up to 21.9 MN/m^2 (3180 lb/in.^{2}).

In the work reported here, we have observed stress–strain relationships of several starch xanthide- and carbon black-reinforced elastomers. The starch xanthide-reinforced elastomers have been prepared under various precipitation conditions, and subsequently, the structure of the dispersed phase in the continuous phase has been characterized.

For carbon blacks, structure is usually measured by dibutyl phthalate ab-

© 1977 by John Wiley & Sons, Inc.

sorption of the bulk filler. For starch xanthide, we have used the transmission electron microscope (TEM) measurement of particle shape in the rubber matrix as a direct measure of structure. These two structure parameters may not correlate directly, however, because the basic unit of their structure differs.

High-structured carbon blacks have complex-shaped particles consisting of reticulated chains of fused primary spherical particles. High-structured starch xanthides have complex-shaped particles consisting of network or branched fibers.

Low-structured samples of both carbon black and starch xanthide are composed of spheroidal or ellipsoidal particles.

We have attempted to correlate particle size and shape of the reinforcing starch xanthide, as determined by TEM, with stress–strain relationships. Comparisons of stress–strain data from carbon black samples with known size and structure were used as a reference.

EXPERIMENTAL

Preparation of Starch Xanthide Masterbatch

Starch xanthide-reinforced vulcanizates were prepared by the method of Buchanan et al.[6] An unmodified corn starch was dispersed in distilled water at about a 10 wt-% level and gelatinized by adding 0.05 mole of NaOH per unit mole of starch. Xanthate degree of substitution (D.S.) was 0.06 produced by the addition of 0.1 mole CS_2 per unit mole of starch.

Rubber latex, starch xanthate solution, antioxidant emulsion (1.25 phr), and sodium nitrite were mixed in a 6-liter Waring Blender. Sodium nitrite was added in a 1:1 mole ratio with the carbon disulfide.

When sulfuric acid was added rapidly to the mixture in varying quantities, various filler particle structures were produced. After the mixture was stirred for several minutes, the serum was drained from the coprecipitates on a vacuum filter. The coprecipitates were washed several times with water. They were dried to 20% moisture in a forced-draft oven at 70°C and then allowed to equilibrate for 18 hr at room temperature in polyethylene bags. The coprecipitates were dried by passing them through a three-zone heated extruder. After three passes, the dried coprecipitates were consolidated on a laboratory mill. All samples contained 43 ± 1 phr starch xanthide filler.

Preparation of Carbon Black Masterbatch

Carbon black samples consisting of two different particle sizes and three different structures each were obtained from Cabot Corporation (Boston, Mass.). These blacks were incorporated into SBR 1502 on a laboratory differential roll mill. All preparations contained 50 phr carbon black.

Compounding and Curing

Starch xanthide- and carbon black-reinforced rubber samples were compounded according to the recipe given in ASTM D15 compound 5C (masterbatch,

143 parts; ZnO, 3 parts; S, 1.75 parts; stearic acid, 1.5 parts; N-*tert*-butyl-2-benzothiazole sulfenamide, 1.25 parts). Mixing was done on a laboratory differential roll mill. Curing characteristics were determined with an oscillating disk rheometer operating with a rotor frequency of 1.67 Hz at an amplitude of ±3°. Samples were cured to t_c' (90%) at a temperature of 150°C. Tensile specimens were cut according to ASTM D412, die C specifications.

Stress Relaxation Measurements

Stress relaxation experiments were carried out with an Instron testing machine at constant temperature (23°C) and constant humidity (50%). Fiduciary points were located about 2.5 cm apart on the specimen, each point being determined as the intersection of two lines at 45° to the test direction. Values of l were measured with a cathetometer reading to 10^{-4} cm. The sample was elongated to a strain ratio $\lambda = l/l_0$, and stress was followed as a function of time, generally over 600 sec. The strain ratio was then increased in steps; relaxation kinetics were followed for 600 sec at each stage.

Bagley and Dixon[5] have shown, for both carbon black- and starch xanthide-reinforced vulcanizates, that double logarithmic plots of load versus time at constant strain are linear over five decades in time, the slope being relatively insensitive to either filler type or loading level. (This linearity makes it possible to compare Mooney-Rivlin[7,8] plots of (load/λ − λ^{-2}) versus λ^{-1} for different systems.)

Dynamic measurements were carried out on an eccentric rotating disk rheometer (Rheometrics Mechanical Spectrometer, Accord, Mass.). True values for displacement (a) and force in the x and y direction (F_x, F_y) were calculated from the instrument compliance (K) by the following equations after Macosko:[9]

$$a_t^2 = a_m^2 - 2a_m K_y F_{ym} + K_y^2 F_{ym}^2 + K_x^2 F_{xm}^2 \tag{1}$$

$$F_{yt} = \frac{F_{ym}}{a_t}\left[a_m - K_y F_{ym} - \left(\frac{K_x F_{xm}^2}{F_{ym}}\right)\right] \tag{2}$$

$$F_{xt} = \frac{F_{xm}}{a_t}\left[a_m - F_{ym}(K_x - K_y)\right] \tag{3}$$

where the subscript t indicates the true values and m indicates measured values.

TABLE I
Physical Properties of SBR 1502, 43 phr Starch Xanthide

Sample no.	Serum pH	Elongation at break, %	Modulus, MN/m²		Tensile strength, MN/m²	Tension set at break, %	Geometric mean particle diameter, μm
			100%	300%			
78	2.86	390	3.65	17.24	21.86	25	0.096
83	4.11	390	5.03	12.55	14.89	34	0.264
88	4.96	430	4.83	9.96	11.65	30	0.274
93	6.03	500	2.69	7.93	12.75	22	0.199

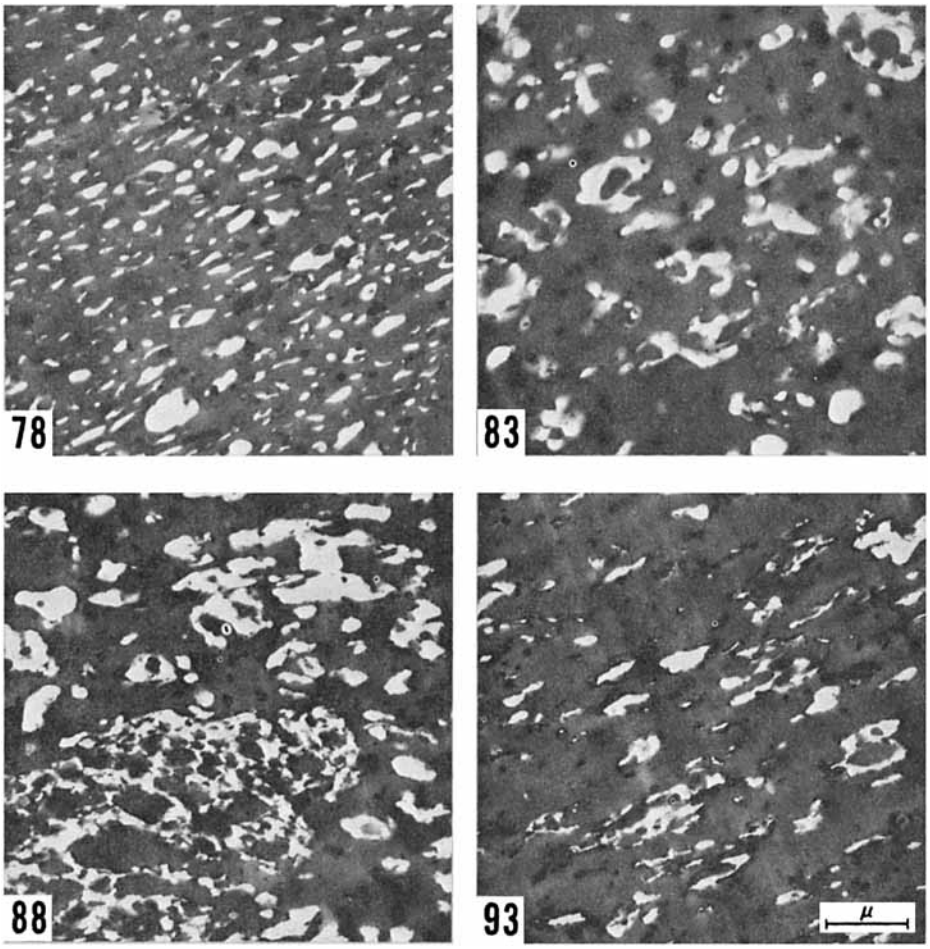

Fig. 1. Transmission electron photomicrographs of starch xanthide–SBR rubbers: sample 78, coprecipitation serum pH 2.86; sample 83, serum pH 4.11; sample 88, serum pH 4.96; sample 93, serum pH 6.03. Light areas are starch particles.

RESULTS AND DISCUSSION

The vulcanizate moduli, elongation, tensile strength, set, and other properties of SBR 1502, reinforced with 43 phr starch xanthide precipitated at four different levels of acid addition, are given in Table I. The 300% modulus shows a substantial decrease from 17.2 to 7.9 MN/m^2 where serum pH, as measured during the coprecipitation, goes from 2.86 to 6.03. Tensile strength in general decreases as pH increases.

In TEM photomicrographs (Fig. 1) of the four samples tabulated in Table I, it can be seen that coprecipitation conditions influence starch xanthide dispersion, particle size, and shape considerably. The starch xanthide particles are of distinctly different types or structures. (Starch xanthide particles appear as light areas in TEM photomicrographs.) Sample 78 is composed of small distinct starch xanthide filler particles (low structure); sample 83 consists of some

irregular, honeycomb, or chain-like particles (medium structure); sample 88 has mostly honeycomb or chain-like particles (high structure); sample 93 is made up of large, but distinct, starch xanthide filler particles.

The photomicrographs in Figure 1, however, do not show average views owing to the small scale used; sample 88 appears to have greater starch xanthide filler area compared to 93. Photomicrographs using a large domain exhibit nearly equal areas of starch xanthide filler.[6]

After observing the photomicrographs carefully, it is convenient to consider the modulus values calculated from the Mooney-Rivlin[7,8] relationship:

$$E_a = f/2(\lambda - \lambda^{-2}) = (L/A_0)/2(\lambda - \lambda^{-2}) \quad (4)$$

where f is the force per unit cross section, L is the load, and A_0 is the area measured in the unstrained state.

The 600-sec apparent modulus (Table II) for samples 78, 83, 88, and 93 are plotted as a function of inverse strain ratio (λ^{-1}) (Fig. 2). For several samples, values for $(L/A_0)/(\lambda - \lambda^{-2})$ rise steeply as λ^{-1} approaches 1. Sample 88, which shows the greatest structure in the photomicrographs, rises the most rapidly as λ^{-1} approaches 1 (estimated limiting slope 3.40). Sample 83, which has medium

TABLE II
Stress Relaxation Data for SBR 1502 at a 43 phr Starch Xanthide Loading Level

Sample no.	Inverse strain ratio λ^{-1}	$(L_{600}/A_0)/(\lambda - \lambda^{-2})$, $(N/m^2)\times10^{-5}$
78	0.96377	18.50
	0.91547	17.51
	0.87312	16.27
	0.78377	14.56
	0.77095	14.66
	0.50597	14.43
	0.39574	18.37
83	0.95530	23.53
	0.93139	22.12
	0.92871	21.66
	0.89959	20.25
	0.85278	18.70
	0.64422	15.14
	0.48933	15.62
88	0.97295	33.90
	0.96212	31.16
	0.94786	30.03
	0.90652	25.63
	0.85866	22.40
	0.85255	22.44
	0.69679	17.50
	0.50464	15.85
93	0.94859	17.00
	0.89405	14.96
	0.98117	14.11
	0.81596	13.39
	0.76894	12.08
	0.72184	12.14
	0.52113	10.62
	0.40790	11.22

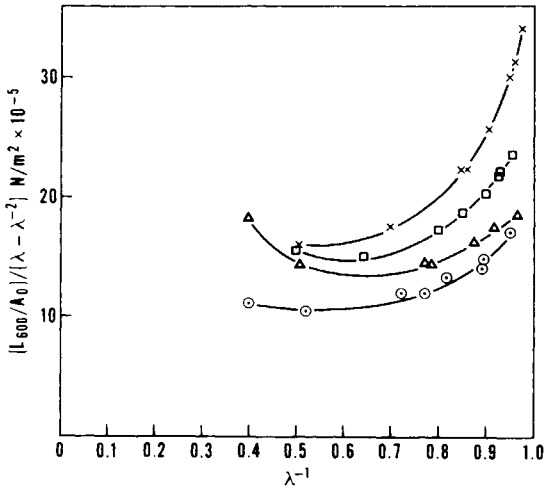

Fig. 2. Mooney-Rivlin plots of 600-sec apparent modulus at 43 phr starch xanthide loading levels in an SBR 1502 vulcanizate: (△) sample 78; (□) sample 83; (x) sample 88; (○) sample 93.

structure, has a moderate rise (estimated limiting slope 1.60), and samples 78 and 93, both classified as having no structure, rise little as λ^{-1} approaches 1 (estimated limiting slope 0.80 and 1.20, respectively). Samples 78 and 93, which differ in particle size but are similar in structure, behave quite alike at low deformation. In view of the other samples of differing structure, the behavior of starch-reinforced rubber vulcanizates at low deformation can be considered a sensitive measure of the filler structure.

From a Mooney-Rivlin plot, however, no difference in behavior could be distinguished at low strain between samples of carbon black of various particle size and particle structure (Table III). Three carbon black samples of varying structure behave similarly throughout the test range (Fig. 3), the only difference being the higher moduli of the most structured black. The order of structure is N-347 > N-330 > N-326. It is unknown at this time why stress–strain behavior at low deformation is independent of the carbon blacks used, which are supposedly of differing structures.

Even though samples 78 and 93 (low-structure, small particles and low-structure, large particles, respectively) show similar behavior at low deformation

TABLE III
Carbon Black Characteristics and Vulcanizate Properties

Carbon black	Particle diameter, nm	Structure parameter[a]	Modulus, MN/m²		Tensile strength, MN/m²
			100%	300%	
N-326	26–30	71	2.21	13.31	24.72
N-330	26–30	102	2.90	17.72	17.93
N-347	26–30	124	3.31	19.89	23.72
N-762	61–100	65	1.93	10.03	18.89
N-765	61–100	112	3.10	15.86	20.31
N-774	61–100	72	2.10	10.24	16.06

[a] Structure parameter for carbon black is dibutyl phthalate number as listed in ASTM D 1765-72.

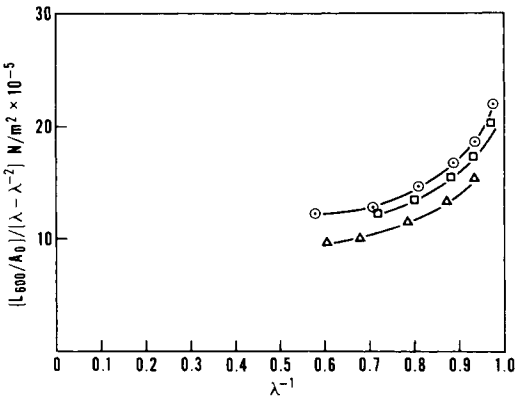

Fig. 3. Mooney-Rivlin plots of 600-sec apparent modulus at 50 phr carbon black loading levels in an SBR 1502 vulcanizate: (△) sample N-326; (□) sample N-330; (○) sample N-347.

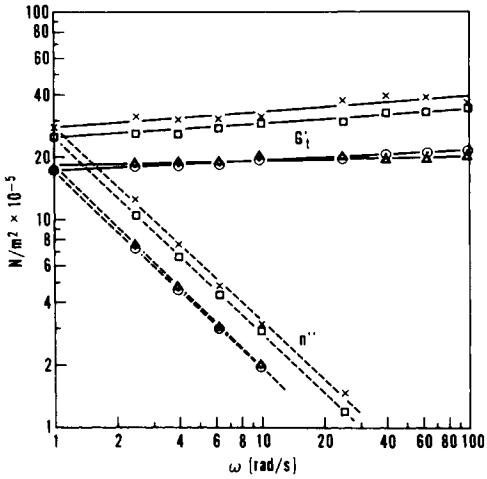

Fig. 4. Storage modulus G_t' and viscosity η'' vs. angular velocity ω for samples with 43 phr starch xanthide loading levels in an SBR 1502 vulcanizate: (△) sample 78; (□) sample 83; (×) sample 88; (○) sample 93.

(Fig. 2), they exhibit greater differences at high deformation. The greater differences at high deformation may be a function of filler particle size. The smaller the particle, the faster the absolute value of the slope of $(L/A_0)/(\lambda - \lambda^{-2})$ versus λ^{-1} increases with increasing strain near fracture. According to Mullins,[10] modulus values at high deformations increase as the number of crosslinks increases. Therefore, one would expect higher modulus values for smaller particles, because the effective crosslink density increases with decreasing filler particle size, the chemical crosslinking being constant in these samples. Samples 83 and 88 have nearly identical particle size and similar modulus values at high deformation. These samples containing highly structured filler particles, however, do not correlate well with samples containing low-structure filler particles at high deformation presumably because of some complex filler interactions.

Apparently, structured starch xanthide reinforcement contributes to high modulus values at low deformation through the starch xanthide network. As deformation increases, the network is broken down, and the interaction between

rigid filler particles and rubber matrix becomes more important, resulting in higher moduli as particle size decreases.[11]

Eccentric Rotating Disk

Dynamic properties of several starch-filled reinforced vulcanizates were determined with an eccentric-rotating disk rheometer (Fig. 4). We have plotted values for the storage modulus (corrected for machine compliance) G_t', as a function of angular velocity ω. The viscosity η'' is also followed as a function of ω.

Both low-structure samples 78 and 93 give nearly identical values of G_t' and η'', whereas samples 83 and 88 show higher storage modulus values with increasing filler structure. Viscosity values also increase as filler structure increases. The eccentric-rotating disk rheometer gives nearly the same qualitative results as stress–strain measurements at low deformation. However, it does not appear to provide as much overall information as static stress–strain tensile tests for the samples studied.

The mention of firm names or trade products does not imply that they are endorsed or recommended by the U.S. Department of Agriculture over other firms or similar products not mentioned.

References

1. R. A. Buchanan, O. E. Weislogel, C. R. Russell, and C. E. Rist, *Ind. Eng. Chem., Prod. Res. Develop.*, **7**, 155 (1968).
2. R. A. Buchanan, H. C. Katz, C. R. Russell, and C. E. Rist, *Rubber J.*, **153**, 28 (1971).
3. H. L. Stephens, R. J. Murphy, and T. F. Reed, *Rubber World*, **161**, 77 (1969).
4. T. P. Abbott, W. M. Doane, and C. R. Russell, *Rubber Age*, **105** (8), 43 (1973).
5. E. B. Bagley and R. E. Dixon, *Trans. Soc. Rheol.*, **18** (3), 371 (1974).
6. R. A. Buchanan, H. L. Seckinger, W. F. Kwolek, W. M. Doane, and C. R. Russell, *J. Elastomers Plast.*, **8**, 82 (1976).
7. M. Mooney, *J. Appl. Phys.*, **11**, 582 (1940).
8. R. S. Rivlin, *Phil. Trans. Roy. Soc. London*, **A241**, 379 (1948).
9. C. W. Macosko, W. M. Davis, *Rheol. Acta*, **13**, 814 (1974).
10. L. Mullins, *J. Appl. Polym. Sci.*, **2**, 257 (1959).
11. R. J. Dennenberg and E. B. Bagley, *J. Appl. Polym. Sci.*, **19**, 519 (1975).

Received November 25, 1975
Revised February 2, 1976